

Formation and Optical Properties of Cylindrical Gold Nanoshells on Silica and Titania Nanorods

Steven J. Limmer, Tammy P. Chou, and Guozhong Cao*

University of Washington, Materials Science and Engineering, 302 Roberts Hall, Box 352120, Seattle, Washington 98195

Received: April 13, 2003; In Final Form: July 21, 2003

Metal–insulator core–shell structures have been demonstrated to have interesting and tunable optical properties. Systems previously investigated include silica-capped gold particles and gold shells surrounding silica particles. However, many of the systems studied so far have been spherical (or zero-dimensional). Thus, it would be of interest to look at the synthesis and optical properties of one-dimensional (i.e., rodlike) nanostructures. In this paper, the authors present and discuss the formation and properties of silica and titania nanorods encapsulated with a thin gold shell. Nanorods of silica and titania $\sim 10 \mu\text{m}$ in length and with diameters $\sim 90\text{--}200 \text{ nm}$ are made by combining sol–gel electrophoresis with a suitable template. After removing the template at high temperature, the surface of the rods is re-hydrolyzed by heating in water. 3-Aminopropyltrimethoxysilane is reacted with the surface hydroxyl groups, self-assembling amine functionality on the surface of the rods. These groups act as anchoring sites for the gold, which forms a thin shell around the oxide nanorod. UV–vis absorbance spectra of these samples are analyzed to determine the relationships between shell thickness, core size, core material, and properties.

Introduction

Nanoscale materials are unquestionably one of the most exciting current research areas, with applications spanning many disciplines. For example, nanomaterials are of great interest for numerous optical applications. This is related to their wide range of novel properties. For example, the photoluminescence behavior of CdSe quantum dots is strongly size-dependent,¹ and TiO₂ nanorods have far better photocatalytic behavior than bulk TiO₂ films.² Researchers have also looked at the optical properties of rodlike or wirelike metal structures, demonstrating the effect of nanorod length on optical properties.³ One particularly interesting area of nanomaterials research is the area of core–shell composite nanostructures, which have a central core of one material surrounded by a shell of a different material. With dimensions of approximately the wavelength of visible light, these core–shell structures can have interesting optical properties.

In addition to synthesizing simple one-component nanostructures, much research has gone into synthesis of multicomponent systems, such as a (nanoscale) core of one material coated with a (nanoscale) shell of another. Systems such as this are referred to as core–shell nanostructures. Numerous spherical core–shell systems have been studied. Researchers have synthesized core–shell quantum dot structures, where a second semiconductor surrounds the central semiconductor material, which yields tunable optical properties.^{4,5} SiO₂-encapsulated Au nanoparticles have been synthesized to show varying absorbance properties.^{6,7} Au-coated TiO₂ nanoparticles, as another example, show slight shifts in absorbance peak with varying TiO₂/Au ratios, and have a distinct improvement in photocatalytic oxidation of thiocyanate.⁸ Au-coated SiO₂ particles have been synthesized to show a large number of properties. SiO₂ particles decorated with small Au clusters show differences in optical properties depending

on the density of coverage.⁹ When the SiO₂ particles are completely covered with Au, it is possible to tune the optical properties over a wide range by varying the core size and shell thickness.^{10–12} For all of these systems, the optical properties depend strongly on the dimensions of the samples. For instance, the inner and outer diameter of Au shells on SiO₂ or the diameter and length of Ag wires control the plasmon energies of the samples. This gives these types of structures essentially tunable optical properties, where control over the physical dimensions of a sample gives the desired behavior.

While much work has been done on spherical core–shell systems, little research has been done on one-dimensional (i.e., rodlike) core–shell structures. Some researchers have synthesized semiconductor core–shell rod structures,¹³ similar to the more common spherical core–shell quantum dot structures. Others have synthesized metal–metal core–shell nanorods,¹⁴ which have differing optical properties from those of nanorods of either the core or shell metal alone. In the area of metal-oxide core–shell systems, one group has described the synthesis of silica-coated gold nanorods,¹⁵ which have differing optical properties from the uncoated gold rods. Another group has made TiO₂-coated Au rods,¹⁶ though they do not mention the optical properties of their product. There is no prior information in the literature about metal shells on oxide nanorods. This chapter discusses the synthesis and analysis of cylindrical nanoshells of Au formed on nanorods of SiO₂ and TiO₂. The template-based synthesis of SiO₂ and TiO₂ nanorods by a combination of sol preparation and electrophoresis is discussed, as well as the formation of a Au layer on the nanorods. Experimental and calculated absorbance spectra are compared for a variety of SiO₂ core diameters and Au shell thicknesses. Some preliminary results for Au shells on TiO₂ cores are also presented.

* Corresponding author. E-mail: gzc@u.washington.edu.

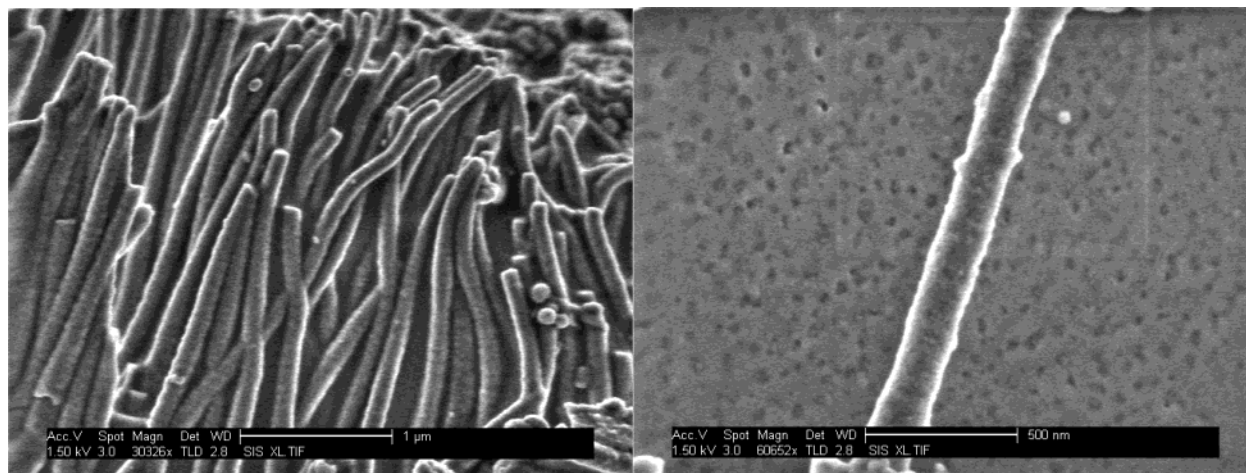


Figure 1. SEM micrographs of Au-coated SiO₂ nanorods. Left, 100 nm SiO₂ with 22 nm of Au. Right, 100 nm SiO₂ with 24 nm of Au.

Experimental Section

The chemicals used in making the sols are titanium(IV) isopropoxide (Alfa Aesar), tetraethyl orthosilicate (Aldrich), hydrochloric acid (Fisher), glacial acetic acid (Fisher), ethanol (Pharmco), and deionized water. For the gold coatings, the chemicals are 3-aminopropyltrimethoxysilane (Aldrich), tetrakis-(hydroxymethyl)phosphonium chloride (Aldrich), hydrogen tetrachloroaurate(III) (Aldrich), potassium hydroxide (J. T. Baker), and sodium borohydride (Aldrich). The template membranes used for the growth of the nanorods were track-etched hydrophilic polycarbonate (Millipore, Bedford, MA), with pore diameters of 100 and 200 nm, and a thickness of 10 μm . Silica sol is prepared by dissolving tetraethyl orthosilicate in a mixture of ethanol and DI water. A small amount of hydrochloric acid is added to the sol to adjust the pH to ~ 3 , and the sol is stirred for 2 h at room temperature. The silica sol thus formed is rather stable, requiring several weeks to gel at room temperature. The surface of SiO₂ nanoclusters in such a sol is negative, since the pH is above the isoelectric point (IEP) of SiO₂ (~ 2). Titania sol is formed by dissolving titanium(IV) isopropoxide in glacial acetic acid, stirring at 400 rpm for 30 min at room temperature. Next, DI water is added to the solution with stirring for an additional 30 min. Upon addition of the water, a white precipitate instantaneously forms; however, the precipitate dissolves and the sol becomes a clear liquid after ~ 5 min of stirring. The TiO₂ sol has a pH ~ 2 and is stable at room temperature for about a week. The surface of TiO₂ particles in this sol is positively charged, since the pH is well below the IEP of TiO₂ (~ 6).

Nanorods of silica and titania are grown in a modified version of the method we have previously described.^{17,18} Briefly, the method is as follows. A track-etched polycarbonate filter membrane is used as the template for nanorod formation. SiO₂ or TiO₂ are deposited into the pores of the template from a sol by electrophoresis. The polycarbonate (PC) membrane and the working electrode are placed in a polypropylene filter holder, and held in place with a silicone gasket. This assembly is placed in contact with the sol. A Pt counter electrode is also placed in the sol, parallel to the working electrode. For the electrophoretic growth, a potential of 5 V is applied between the electrodes, and held for 15–60 min. At the end of the electrophoretic deposition, excess sol is blotted off the membrane. Samples prepared in this manner are dried at ~ 100 °C for several hours, then placed in an oven and fired in air at 500 °C for 1 h. This is to burn off the polycarbonate membranes and increase the density of the nanorods.

Gold coatings on the nanorods are formed in a manner similar to that of ref 10. The as-synthesized nanorods are suspended in DI water and boiled at 100 °C for ~ 2 h to re-hydrolyze their surface. Boiling silica has been demonstrated to be an effective means of re-hydrolyzing SiO₂ surfaces for the formation of silane self-assembled monolayers.¹⁹ This is required for the self-assembly process to work. When the nanorods are first synthesized (before firing), there are a large number of hydroxide groups on the nanorod surface. However, these groups are removed (via condensation reactions) upon firing, so it is necessary to reintroduce them to the nanorod surface.

These re-hydrolyzed nanorods are dried to remove excess water, and re-suspended in ethanol. A small amount of 3-aminopropyltrimethoxysilane (APTMS) is added to this suspension. The methoxy groups on the APTMS undergo hydrolysis and condensation reactions with the hydroxyl groups on the nanorod surface to yield the amine-functionalized nanorods. After allowing the APTMS to react for ~ 24 h, the suspensions are centrifuged and rinsed 4 times to remove excess reactants.

To direct the deposition of gold from a solution, small seed particles of gold are first attached to the amine-functionalized nanorods. The seed particles used are from a Au colloidal sol.²⁰ Briefly, this sol is created by reducing a solution of chloroauric acid and NaOH with tetrakis(hydroxymethyl)phosphonium chloride (THPC). This yields a sol of colloidal Au particles of ~ 2 nm. This sol is mixed with the APTMS-coated oxide nanorods, and left for several hours to allow complete attachment of the Au particles to the nanorods.

Once the Au nanoparticles are completely attached to the nanorods, a coating of Au is formed by reducing a 5 mM solution of HAuCl₄ with 1 mM NaBH₄,⁸ using a varying amount of solution to control the gold shell thickness. The Au seeds attached to the nanorod surface act as nucleation sites for the gold being reduced from solution, so the gold is preferentially deposited on the nanorod surface, rather than heterogeneously nucleating large Au particles in the solution. The gold coating forms over a time span from hours to days, depending on the concentration of the suspension, and the amount of Au and NaBH₄ used. Absorbance measurements of some samples show a shift with aging. For example, one sample showed a shift of 5 nm in peak position after 8 days aging, and remained constant for an additional 3 weeks.

Figure 1 shows micrographs of two sets of the Au-coated nanorods. These images demonstrate the final thickness of the Au-nanorod assembly. Because the samples were not sputtered with a conductive layer prior to FE-SEM analysis, no correction

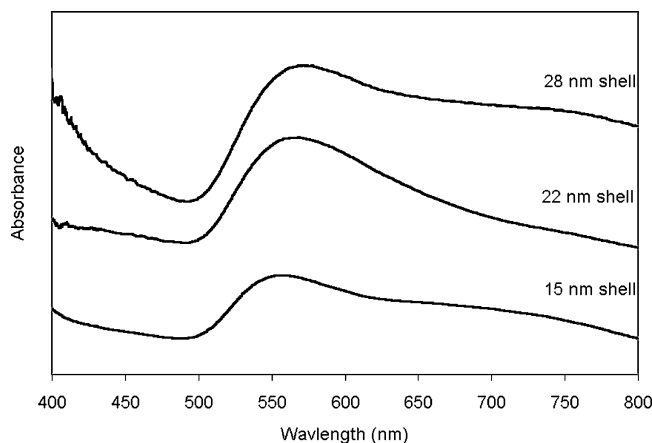


Figure 2. Absorbance spectra for Au-coated 100 nm SiO₂ nanorods.

TABLE 1: Combinations of Oxide Core Diameter and Au Shell Thickness Studied

core material	core diameter (nm)	au shell thickness (nm)
SiO ₂	100	31
SiO ₂	100	29
SiO ₂	100	28
SiO ₂	100	24
SiO ₂	100	23
SiO ₂	100	22
SiO ₂	100	21
SiO ₂	100	15
SiO ₂	200	34
SiO ₂	200	32
SiO ₂	200	13
SiO ₂	200	12
SiO ₂	200	6
TiO ₂	180	4
TiO ₂	90	27

to the measured diameters was needed. From these images, one can also see that the coverage of gold is nearly uniform over the entire length of the nanorods, although there are some scattered “bumps” where the Au is thicker. This technique was used to determine the Au shell thickness for all of the samples. Table 1 lists the combinations of oxide core diameter and Au shell thickness used in this study.

Results and Discussion

The most interesting properties of metal–insulator core–shell systems such as this are in their optical responses. Thus, all of the suspensions of gold-coated nanorods were characterized with UV–Vis absorbance spectroscopy. The absorbance spectra were also calculated to determine if the observed behavior was truly due to the gold coatings as expected.

For analysis, suspensions of Au-coated nanorods in a mixture of ethanol and water were used. The absorbance spectra were recorded with a UV–Vis spectrometer (Ocean Optics PC2000) using a tungsten–halogen light source (Ocean Optics LS-1).

Figure 2 is a comparison of absorbance spectra for three of the 100 nm SiO₂ nanorods coated with varying amounts of gold. In these samples, the absorbance peak decreases from 571 nm for a 28 nm shell, to 568 nm for a 22 nm shell, to 557 nm for a 15 nm shell. The spectra for a selection of 200 nm diameter SiO₂ cores are shown in Figure 3. For these, the absorbance peak decreases from 581 nm for a 34 nm shell, to 550 nm for a 12 nm shell, to a broad shoulder near ~520 nm for a 6 nm shell. Some of the peak breadth in these spectra may be due to the slight spread in size of the nanorods. While they are all ~10 μm in

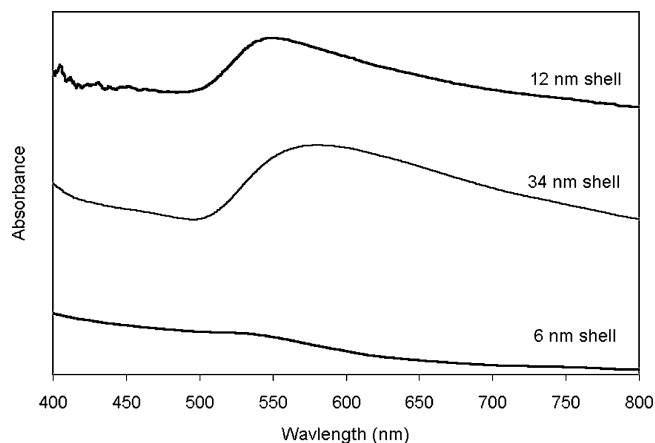


Figure 3. Absorbance spectra for Au-coated 200 nm SiO₂ nanorods.

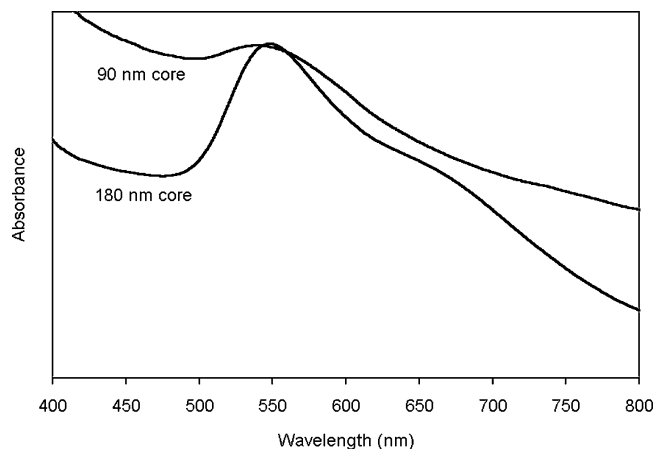


Figure 4. Absorbance spectra for Au-coated TiO₂ nanorods.

length when synthesized, some nanorods do break during sonication or stirring. Since the length of the rod does have a small effect on the absorbance properties, the broken rods broaden the absorbance peak somewhat. As concentrations of the various nanorod suspensions were not constant, all spectra have slight differences in peak intensity.

Because of the difference in dielectric constant between SiO₂ and anatase (about 2.1 and 6.3, respectively),²¹ it is expected that these rods will have somewhat different peak positions for the same core–shell ratios. Figure 4 shows the preliminary data for these rods, comparing the spectra for two TiO₂ nanorod samples. The 180 nm diameter rods coated with 4 nm of Au show a peak at 548 nm, and the 90 nm diameter rods with a 27 nm shell have a peak at 536 nm.

It is known that the absorbance behavior of metal nanorods can be modeled by Mie scattering theory, considering them as prolate spheroids with the given length and maximum diameter.²² A similar model has also been shown for SiO₂ on Au nanorod core–shell structures.¹⁵ This model should also be applicable for the Au on SiO₂/TiO₂ nanorods used in this study. Because core–shell nanorods are 1-D nanostructures, their optical properties are a combination of both nanosize and bulk effects. Along the radial dimension of these structures, the behavior is constrained by the size, while along the length (assuming a large enough aspect ratio) the properties are like that of a bulk material,³ an assumption that simplifies the scattering model. The Drude-Lorentz-Sommerfeld model for the dielectric function can be used for the longitudinal dielectric properties of the nanorod,²³ incorporating the interband portion fitted from the bulk optical properties of Au.²¹ Along the radial direction, however, the Drude model also needs to include a

modified electron mean free path, to account for the gold shell thickness.²³ Using these dielectric functions and the appropriate shape factors for a rodlike geometry in the polarizability equation for a core-shell system allows one to calculate the scattering behavior of the Au-coated nanorods. Combining all of these considerations leads to the equations for the calculated absorbance.

The mean absorption cross section for prolate spheroids, when averaged over all orientations, is calculated by²⁴

$$\sigma(\lambda) = \frac{2\pi\epsilon_m^{1/2}}{\lambda} \text{Im}[\alpha_l + 2\alpha_t] \quad (1)$$

where α_l and α_t are the longitudinal and transverse polarizabilities, respectively. They are functions of the core, shell, and matrix (complex) dielectric constants. In the case of a prolate core-shell structure, the polarizabilities are given by¹⁵

$$\alpha_{l,t} = \frac{V(\epsilon_s - \epsilon_m)\{\epsilon_s + [(\epsilon_c - \epsilon_s)(P_{lt}^1 - P_{lt}^2)]\} + f\epsilon_s(\epsilon_c - \epsilon_s)}{[\epsilon_s + (\epsilon_c - \epsilon_s)(P_{lt}^1 - fP_{lt}^2)][\epsilon_m + (\epsilon_s - \epsilon_m)P_{lt}^2] + fP_{lt}^2\epsilon_s(\epsilon_c - \epsilon_s)} \quad (2)$$

where V is the total (core plus shell) volume per particle and f is the volume fraction of the core. The four values of P are the depolarization factors, where the superscripts 1 and 2 refer to the core and shell, respectively, while the subscripts l and t are for the longitudinal and transverse modes. With r the core radius, l the particle length, and t_s the Au shell thickness, these depolarization values are calculated from²⁵

$$P_l^1 = \frac{1 - e_c^2}{e_c^2} \left[\frac{1}{2e_c} \ln \left(\frac{1 + e_c}{1 - e_c} \right) \right] \quad (3)$$

$$P_t^1 = \frac{1 - P_l^1}{2} \quad (4)$$

$$P_l^2 = \frac{1 - e_s^2}{e_s^2} \left[\frac{1}{2e_s} \ln \left(\frac{1 + e_s}{1 - e_s} \right) \right] \quad (5)$$

$$P_t^2 = \frac{1 - P_l^2}{2} \quad (6)$$

The e values are shape factors, and are calculated for the core (c) and shell (s) as¹⁵

$$e_c^2 = 1 - r^2 / \left(\frac{l}{2} \right)^2 \quad (7)$$

$$e_s^2 = 1 - \frac{(r + t_s)^2}{\left(\frac{l}{2} + t_s \right)^2} \quad (8)$$

Calculations were done assuming a nanorod length of 10 μm . Despite the fact that some of the rods were observed to be shorter than assumed, the calculated data give a good fit to experimental. This is because the length does not have a strong influence on the calculated absorbance. For instance, assuming a length of 5 μm in the calculation for 32 nm of Au on 200 nm SiO₂ only shifts the peak position ~ 4 nm. Table 2 lists a

TABLE 2: Comparison of the Observed and Calculated Peak Positions for Au-Coated SiO₂ Nanorods

sample	observed peak position (nm)	calculated peak position (nm)
31 nm Au/100 nm SiO ₂	577	596
29 nm Au/100 nm SiO ₂	572	586
28 nm Au/100 nm SiO ₂	571	581
24 nm Au/100 nm SiO ₂	576	562
23 nm Au/100 nm SiO ₂	557	557
22 nm Au/100 nm SiO ₂	568	553
21 nm Au/100 nm SiO ₂	548	546
15 nm Au/100 nm SiO ₂	557	520
34 nm Au/200 nm SiO ₂	581	527
32 nm Au/200 nm SiO ₂	579	522
13 nm Au/200 nm SiO ₂	577	472
12 nm Au/200 nm SiO ₂	550	470
6 nm Au/200 nm SiO ₂	broad shoulder near ~ 520	459

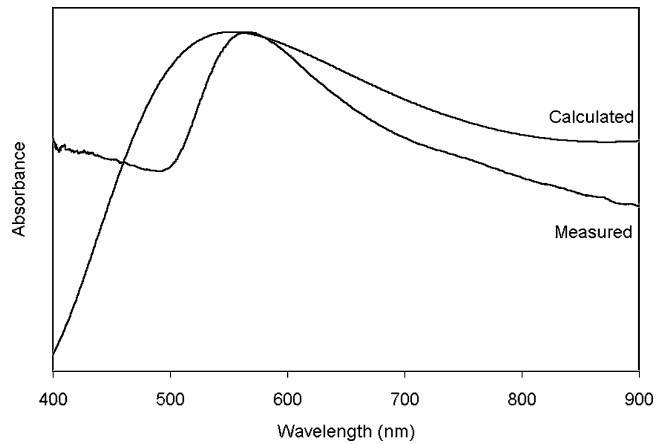


Figure 5. Comparison of the experimental and calculated absorbance spectra for 100 nm SiO₂ nanorods coated with 22 nm of Au.

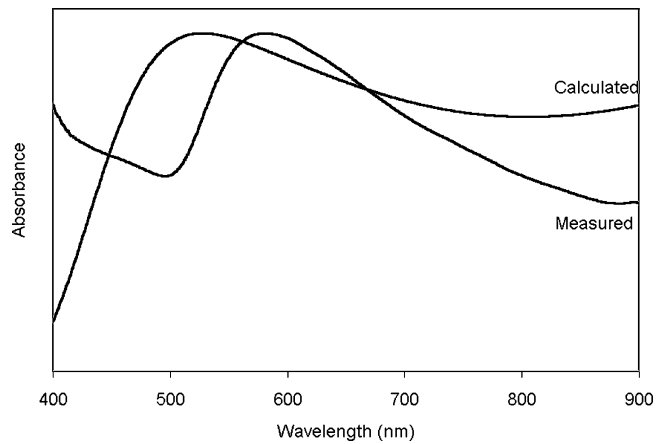


Figure 6. Comparison of the experimental and calculated absorbance spectra for 200 nm SiO₂ nanorods coated with 34 nm of Au.

comparison of the calculated and observed peak positions for all the SiO₂ samples in this study.²⁶

Figures 5 and 6 compare the experimental and calculated absorbance spectra for 22 nm Au/100 nm SiO₂ and 34 nm Au/200 nm SiO₂ samples, respectively, showing the good fit of the calculated spectra to the observed ones. Figure 7 compares the experimental and calculated absorbance spectra for 180 nm TiO₂ cores with a 4 nm Au shell thickness, showing the good fit of the calculated spectra to the observed one.

From Table 2, one can observe some trends in the absorbance behavior of the SiO₂ samples. First, for a given core diameter, the absorbance peak wavelength (both observed and calculated) increases as the shell thickness increases. However, for a given

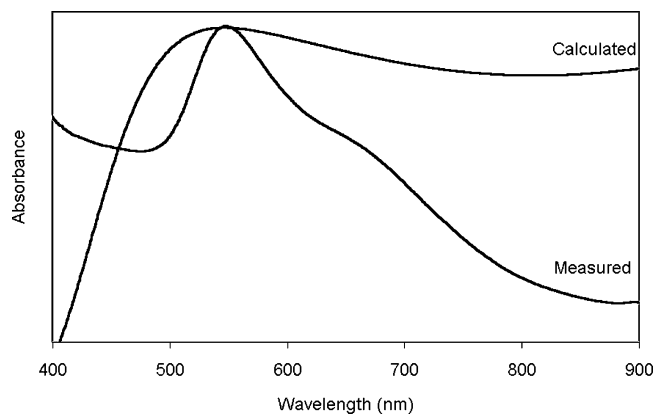


Figure 7. Comparison of the experimental and calculated absorbance spectra for 180 nm TiO₂ nanorods coated with 4 nm of Au.

ratio of core thickness to shell diameter, the value of the peak position is roughly the same, regardless of the core diameter. This is true for both the calculated and measured values. For example, 100 nm SiO₂ rods coated with 15 nm of Au have observed and calculated peak positions of 557 and 520 nm, respectively. This is very close to the values for 200 nm SiO₂ coated with 32 nm Au (core/shell ratio of 0.16) of 579 nm observed and 522 nm calculated. Similar results are seen for all SiO₂ samples. In addition, the difference between observed and calculated positions is larger for 200 nm cores than for 100 nm SiO₂.

There are a few explanations for the discrepancies between the calculated and observed spectra. First, it is assumed that all the core-shell structures are uniform in size. However, there is a certain amount of spread in the core diameters, which could lead to a certain amount of peak broadening/shifting. Similarly, there is likely a spread of lengths of the structures, which would have a small effect on the observed spectra.

For samples with very thin shells, it is quite likely that the coverage of the nanorod is incomplete. Halas et al. have noticed that it is difficult or impossible to achieve complete Au shells of less than ~10 nm thickness on SiO₂ nanoparticles.¹⁰ Thus, the wider discrepancies seen in the thinnest shells (6 nm Au/200 nm SiO₂ and 4 nm Au/180 nm TiO₂) is likely due to the formation of incomplete shells.

It is possible that when the spectra were recorded, the core-shell structures were not well dispersed in the solution. If there were clusters of the nanorods in the liquid (agglomerated by van der Waals interactions, for example), that would alter the absorbance observed, as coupling between the structures shifted the absorbance peak to higher wavelengths. A similar problem would be the existence of bundles of nanorods completely enclosed in Au. While this was not observed in the SEM, it may have occurred, and would further shift the absorbance behavior.

Last, there are potentially some slight difficulties with the model itself. The interband terms used were fitted from real data to a sixth order polynomial, which may not have accurately captured all of the behavior of the dielectric constant of gold over the wavelength interval of interest. In addition, the dielectric constant used for the medium is an approximate value for a mixture of ethanol and water. It is known that higher values of the medium dielectric constant will shift the absorbance peak to higher wavelengths. While this value has only a slight effect on the calculated values, when combined with the other factors mentioned above, it might contribute somewhat to the discrepancies noted. In the calculated spectra for TiO₂ cores, the dielectric function used for TiO₂ was not completely accurate.

First, while the value used (6.3) is correct for bulk anatase, amorphous, poorly crystalline or porous samples (which is the case here) can have dielectric constants as low as 4 or 5.^{27,28} Additionally, anatase TiO₂ is a semiconductor with a band-gap of about 3.2 eV,²⁹ or ~390 nm. Thus, there is a strong absorbance due to TiO₂ at lower wavelengths, which is not accounted for in the model.

Conclusions

Through a combination of sol-gel chemistry, electrophoresis, and self-assembly, it is possible to grow oxide nanorods with a thin shell of gold on their surface. By varying the diameter of the oxide rods and the thickness of the Au coating, it is possible to tune the optical properties of these structures. For instance, changing from a 100 nm SiO₂ nanorod with 31 nm of Au coating to a 200 nm rod with 32 nm of Au induces a shift in the absorbance peak from 577 to 579 nm. Similarly, changing the thickness of Au coating on 100 nm SiO₂ nanorods from 15 to 31 nm shifts the absorbance peak from 557 to 577 nm. Changing the core material can also alter the optical properties of these core-shell structures. This can be seen in a change from SiO₂ (with a dielectric constant of ~2.1) to anatase TiO₂ (with a dielectric constant of ~6.3). Also, 200 nm SiO₂ nanorods with 6 nm of Au have an absorbance shoulder near 525 nm, where 180 nm TiO₂ nanorods with 4 nm of Au have a peak at 548 nm.

These results suggest that the formation of a general class of oxide-metal core-shell systems should be possible, giving 4 degrees of freedom in tuning the optical properties: core material, core diameter, shell material, and shell thickness. Already a wide variety of core oxides can be formed into nanorods by sol electrophoresis. These nanorods could be easily functionalized to have amine or thiol groups on their surfaces to bind with the desired metal. Last, a metal can be chosen from the number that can be synthesized as colloids and chemically deposited (such as Au, Ag, and Pt).

The absorbance spectra of the core-shell structures synthesized can also be calculated using Mie scattering theory. It was found that all but one sample followed the calculated trend of increasing absorbance peak position with increasing Au shell thickness. The calculated spectra show good agreement with the measured results. For example, in the SiO₂ nanorods, there was an average difference of about 24 nm between the observed and calculated spectra.

Acknowledgment. S.J.L. thanks the Ford Motor Company fellowship and the NSF-IGERT fellowship from the center for nanotechnology at the University of Washington for support. T.P.C. acknowledges support from the Joint Institute for Nanoscience funded by the Pacific Northwest National Laboratory (operated by Battelle for the U.S. Department of Energy) and the University of Washington.

References and Notes

- (1) Ramsden, J. J.; Graetzel, M. *J. Chem. Soc., Faraday Trans. 1* **1984**, 80, 919.
- (2) Hulstee, J. C.; Martin, C. R. *J. Mater. Chem.* **1997**, 7, 1075.
- (3) Sun, Y.; Gates, B.; Mayers, B.; Xia, Y. *Nano Lett.* **2002**, 2, 165.
- (4) Dabbousi, B. O.; Rodriguez-Viejo, J.; Mikulec, F. V.; Heine, J. R.; Mattoussi, H.; Ober, R.; Jensen, K. F.; Bawendi, M. G. *J. Phys. Chem. B* **1997**, 101, 9463.
- (5) Yoffe, A. D. *Adv. Phys.* **2001**, 50, 1.
- (6) Hall, S. R.; Davis, S. A.; Mann, S. *Langmuir* **2000**, 16, 1454.
- (7) Caruso, F.; Spasova, M.; Salgueiriño-Maceira, V.; Liz-Marzán, L. M. *Adv. Mater.* **2001**, 13, 1090.
- (8) Dawson, A.; Kamat, P. V. *J. Phys. Chem. B* **2001**, 105, 960.

- (9) Westcott, S. L.; Oldenburg, S. J.; Lee, T. R.; Halas, N. J. *Langmuir* **1998**, *14*, 5396.
- (10) Oldenburg, S. J.; Averitt, R. D.; Westcott, S. L.; Halas, N. J. *Chem. Phys. Lett.* **1998**, *288*, 243.
- (11) Oldenburg, S. J.; Hale, G. D.; Jackson, J. B.; Halas, N. J. *Appl. Phys. Lett.* **1999**, *75*, 1063.
- (12) Oldenburg, S. J.; Jackson, J. B.; Westcott, S. L.; Halas, N. J. *Appl. Phys. Lett.* **1999**, *75*, 2897.
- (13) Manna, L.; Scher, E. C.; Li, L.-S.; Alivisatos, A. P. *J. Am. Chem. Soc.* **2002**, *124*, 7136.
- (14) Ah, C. S.; Hong, S. D.; Jang, D.-J. *J. Phys. Chem. B* **2001**, *105*, 7871.
- (15) Shih, C.-W.; Lai, W.-C.; Hwang, C.-C.; Chang, S.-S.; Wang, C. R. C. Electrochemical synthesis and optical properties of gold nanorods. In *Metal Nanoparticles*; Feldham, D. L., Foss, C. A., Jr., Eds.; Marcel Dekker: New York, 2002; p 163.
- (16) Guo, Y.-G.; Wan, L.-J.; Bai, C.-L. *J. Phys. Chem. B* **2003**, *107*, 5441.
- (17) Limmer, S. J.; Seraji, S.; Forbess, M. J.; Wu, Y.; Chou, T. P.; Nguyen, C.; Cao, G. Z. *Adv. Mater.* **2001**, *13*, 1269.
- (18) Limmer, S. J.; Seraji, S.; Wu, Y.; Chou, T. P.; Nguyen, C.; Cao, G. Z. *Adv. Funct. Mater.* **2002**, *12*, 59.
- (19) Feng, X.; Fryxell, G. E.; Wang, L.-Q.; Kim, A. Y.; Liu, J.; Kemner, K. M. *Science* **1997**, *276*, 923.
- (20) Duff, G.; Baiker, A.; Edwards, P. P. *Langmuir* **1993**, *9*, 2301.
- (21) *CRC Handbook of Chemistry and Physics*, 74th ed.; Lide, D. R., Ed.; CRC Press: Boca Raton, FL, 1994; pp 12–113.
- (22) Link, S.; El-Sayed, M. A. *Int. Rev. Phys. Chem.* **2000**, *19*, 409.
- (23) Kreibig, U.; Vollmer, M. *Optical Properties of Metal Clusters*, Springer-Verlag: Berlin, 1995; pp 14–19.
- (24) Bohren, C. F.; Huffman, D. R. *Absorption and Scattering of Light by Small Particles*; Wiley: New York, 1983.
- (25) Creighton, J. A.; Eadon, D. G. *J. Chem. Soc., Faraday Trans.* **1991**, *87*, 3881.
- (26) A preliminary version of these calculations was included in Limmer, S. J.; Chou, T. P.; Cao, G. Z. *ProcSPIE – Int. Soc. Opt. Eng.* **2002**, *4809*, 222. However, an incorrect formulation was used for the interband portion of the dielectric constant of Au. This has been corrected in the present paper.
- (27) Mardare, D.; Hones, P. *Mater. Sci. Eng. B* **1999**, *68*, 42.
- (28) Won, D.-J.; Wang, C.-H.; Jang, H.-K.; Choi, D.-J. *Appl. Phys. A* **2001**, *73*, 595.
- (29) Mosaddeq-ur-Rahman, M.; Yu, G.; Krishna, K. M.; Soga, T.; Watanabe, J.; Jimbo, T.; Umeno, M. *Appl. Opt.* **1998**, *37*, 691.